Spectral Fraunhofer regime: time-to-frequency conversion by the action of a single time lens on an optical pulse

José Azaña, Naum K. Berger, Boris Levit, and Baruch Fischer

We analyze a new regime in the interaction between an optical pulse and a time lens (spectral Fraunhofer regime), where the input pulse amplitude is mapped from the time domain into the frequency domain (time-to-frequency conversion). Here we derive in detail the conditions for achieving time-to-frequency conversion with a single time lens (i.e., for entering the spectral Fraunhofer regime) as well as the expressions governing this operation. Our theoretical findings are demonstrated both numerically and experimentally. A comparative study between the proposed single-time-lens configuration and the conventional dispersion + time-lens configuration for time-to-frequency conversion is also conducted. Time-to-frequency conversion with a single time lens can be used for applications similar to those previously proposed for the conventional time-to-frequency converters, e.g., high-resolution measurement of fast optical temporal waveforms. Moreover, our results also indicate that the spectral Fraunhofer regime provides additional capabilities for controlling and processing optical pulses.

OCIS codes: 070.2590, 320.5540, 060.5060, 200.3050, 250.5530.

1. Introduction

Space–time duality is based on the analogy between the equations that describe the paraxial diffraction of beams in space and the first-order temporal dispersion of optical pulses in a dielectric.[1–8] The duality can also be extended to consider imaging lenses: The use of quadratic phase modulation on a temporal waveform is analogous to the action of a thin lens on the transverse profile of a spatial beam.[1–7] The time lens can be implemented in practice with an electro-optic phase modulator driven by a sinusoidal radio frequency (RF) signal,[2,4,6] by mixing the original pulse with a chirped pulse in a nonlinear crystal[3,5] (sum-frequency generation), or by means of cross-phase modulation of the original pulse with an intense pump pulse in a nonlinear fiber.[7] Optical signal processing operations based on a time lens include real-time Fourier transformation,[1,6] temporal imaging,[2,3] and time-to-frequency conversion.[4–7]

Here we conduct a detailed investigation of a new regime in the interaction between optical pulses and time lenses. In particular, we demonstrate that when a time lens operates on an optical pulse this pulse can enter a regime where the input pulse amplitude is mapped from the time domain into the frequency domain (time-to-frequency conversion). As is schematically shown in Fig. 1, this regime can be interpreted as the frequency-domain dual of the temporal Fraunhofer regime[8] (frequency-to-time conversion or real-time Fourier transformation by temporal dispersion) and, as a result, we refer to it as the spectral Fraunhofer regime.

Among other potential applications, time-to-frequency conversion can be used for the measurement of the intensity temporal profile of ultrashort optical pulses (by simply measuring the spectrum of the transformed signal). In contrast with other approaches, time-to-frequency conversion provides a fast, noniterative (single-shot) and unambiguous measurement of the temporal waveform, being especially suited for the measurement of long single-transient events with ultrafast temporal details or, equivalently, signals with a large time–bandwidth product. Time-to-frequency conversion was previ-

J. Azaña (azana@inrs-emt.uquebec.ca) is with the Institut National de la Recherche Scientifique (INRS)—Énergie, Matériaux et Télécommunications, 800 de la Gauchetière Ouest, Suite 6900, Montréal, Québec H5A 1K6, Canada. N. K. Berger, B. Levit, and B. Fischer (fischer@ee.technion.ac.il) are with the Department of Electrical Engineering, Technion—Israel Institute of Technology, Haifa 32000, Israel.

Received 15 May 2003; revised manuscript received 19 September 2003; accepted 14 October 2003.

0003-6935/04/020483-08$15.00/0

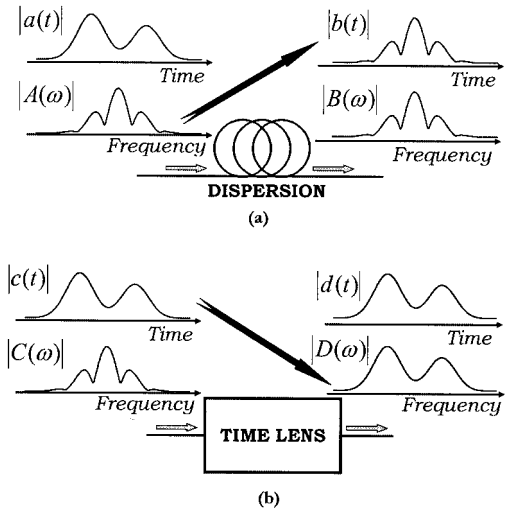

Fig. 1. Dual Fraunhofer regimes: (a) frequency-to-time conversion using dispersion, (b) time-to-frequency conversion using a single time lens.

ously demonstrated with a system comprising a time lens preceded by a suitable dispersive device[4–7] (schematic shown in Fig. 2). Our proposal (using a single time lens operating in the spectral Fraunhofer regime) simplifies the design and implementation of time-to-frequency converters, since it avoids the use of a dispersive device preceding the time lens.

In this paper we derive the conditions for achieving time-to-frequency conversion with a single time lens (i.e., conditions for entering the spectral Fraunhofer regime) as well as the expressions governing this operation. Our theoretical findings are confirmed by means of numerical simulations, and an experimental demonstration of the phenomenon is also provided. A comparative study between the single-lens configuration and the dispersion–time-lens configuration for time-to-frequency conversion is also completed.

2. Theory

A. Temporal Fraunhofer Regime in a Dispersive Medium

As is shown in Fig. 1, the spectral Fraunhofer regime in a time lens can be interpreted as the frequency-domain dual of the temporal Fraunhofer regime (real-time Fourier transformation) in a dispersive medium. We first briefly review the theory of temporal Fraunhofer in dispersive media.[8] In what follows, the involved signals are assumed to be spectrally centered at the optical frequency ω_0; we work with the complex temporal envelope of the signals, and we ignore the average delay introduced by the components (dispersion or time lens). The temporal Fraunhofer regime can be observed when an optical pulse is temporally stretched by first-order dispersion. The first-order dispersion coefficient of the dispersive medium is defined as $\ddot{\Phi}_\omega = [\partial^2\Phi(\omega)/\partial\omega^2]_{\omega=0}$, where $\Phi(\omega)$ is the spectral phase response of the medium. Notice that the variable ω is the baseband frequency variable, i.e., $\omega = \omega_{opt} - \omega_0$, where ω_{opt} is the optical frequency variable. If this dispersion coefficient $\ddot{\Phi}_\omega$ satisfies the condition[8]

$$|\ddot{\Phi}_\omega| \gg \Delta t^2/8\pi, \tag{1}$$

Δt being the total duration of the unstretched optical pulse, then the output pulse envelope $b(t)$ is proportional to the spectrum of the input pulse $A(\omega)$ [see Fig. 1(a)], i.e. $|b(t)| \propto |A(\omega = t/\ddot{\Phi}_\omega)|$. Inequality (1) is usually referred to as the temporal Fraunhofer condition, since it is the time-domain analog of the well-known Fraunhofer condition in the problem of spatial diffraction.

B. Spectral Fraunhofer Regime in a Time Lens

A time lens is a phase-only modulator with a phase modulation function[2]

$$m(t) = \exp[j\phi(t)] \propto \exp[j(\ddot{\phi}_t/2)t^2], \tag{2}$$

where $\ddot{\phi}_t = [\partial^2\phi(t)/\partial t^2]_{t=0}$ will be referred to as the phase-factor of the time lens. Let us now evaluate the action of the time lens over a given arbitrary optical pulse $c(t)$. The output pulse $d(t)$ from the time lens in response to the input pulse $c(t)$ is given by $d(t) = c(t)m(t)$. In the frequency domain, the product can be described as a convolution $D(\omega) = C(\omega) * M(\omega)$, where $D(\omega)$ and $C(\omega)$ are the Fourier transforms of $d(t)$ and $c(t)$, respectively, and $M(\omega)$ is the Fourier transform of the time-lens modulation function, $M(\omega) \propto \exp[-j(1/2\ddot{\phi}_t)\omega^2]$. We derive

$$\begin{aligned} D(\omega) = C(\omega) * M(\omega) &\propto \int_{\Delta\omega} C(\Omega)\exp[-j(1/2\ddot{\phi}_t)(\omega \\ &\quad - \Omega)^2]\mathrm{d}\Omega \propto M(\omega)\int_{\Delta\omega} C(\Omega)\exp[-j(1/2\ddot{\phi}_t)\Omega^2] \\ &\quad \times \exp[j(1/\ddot{\phi}_t)\omega\Omega]\mathrm{d}\Omega, \end{aligned} \tag{3}$$

where $\Delta\omega$ is the total spectral bandwidth of the input pulse $c(t)$. If this bandwidth is sufficiently narrow that it satisfies the condition

$$|\ddot{\phi}_t| \gg \Delta\omega^2/8\pi, \tag{4}$$

then the phase term $\exp[-j(1/2\ddot{\phi}_t)\Omega^2]$ within the last integral in relation (3) can be neglected, since $|(1/2\ddot{\phi}_t)\Omega^2| < (1/2|\ddot{\phi}_t|)(\Delta\omega/2)^2 \ll \pi$ (we remind the

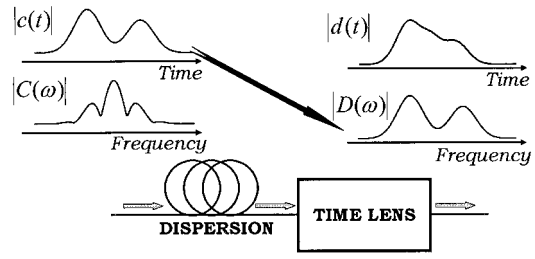

Fig. 2. Schematic of the dispersion–time-lens configuration for time-to-frequency conversion.

reader that the variable Ω is a base-band frequency). In this case, relation (3) can be approximated by

$$D(\omega) \propto M(\omega) \int_{\Delta\omega} C(\Omega)\exp[j(1/\ddot{\phi}_t)\omega\Omega]\mathrm{d}\Omega = M(\omega)c(t = \omega/\ddot{\phi}_t), \quad (5)$$

where the last integral has been solved by considering $\exp[j(1/\ddot{\phi}_t)\omega\Omega]$ the kernel of a Fourier transformation. Relation (5) indicates that under the conditions of inequality (4) the spectrum of the output pulse $D(\omega)$ is, within a phase factor $M(\omega)$, proportional to the input temporal waveform $c(t)$ evaluated at the instant $t = \omega/\ddot{\phi}_t$. In other words, the spectral energy distribution of the output optical pulse $|D(\omega)|^2$ is an image of the temporal intensity distribution of the input optical pulse $|c(t)|^2$, i.e., $|D(\omega)|^2 \propto |c(t = \omega/\ddot{\phi}_t)|^2$ [as represented in Fig. 1(b)]. Inequality (4) is the frequency-domain dual of the temporal Fraunhofer condition in inequality (1). We refer to this inequality as the spectral Fraunhofer condition. Note that inequality (4) conditions the phase-factor (chirp) of the time lens $|\ddot{\phi}_t|$, depending on the fastest temporal feature of the input optical signal to be measured, $\delta t \approx 2\pi/\Delta\omega$ (i.e., depending on the required temporal resolution δt). Specifically, according to inequality (4), the shorter (faster) the temporal feature to be resolved, the larger the phase factor of the time lens must be. In particular, an estimation of the temporal resolution δt provided by the system can be obtained from inequality (4) by simple mathematical manipulation. We first derive that $|\ddot{\phi}_t| \gg (2\pi/\delta t)^2/8\pi \approx \pi/(2\delta t^2)$, which translates into a condition for the shorter temporal feature that can be resolved by the system, $\delta t^2 \gg \pi/(2|\ddot{\phi}_t|)$. Strictly, this condition can be written as

$$\delta t > \sqrt{5\pi/|\ddot{\phi}_t|} \approx 4/\sqrt{|\ddot{\phi}_t|}. \quad (6)$$

However, our experimental and simulation results have demonstrated that this condition is too restrictive, much as the similarly derived Fraunhofer-zone distance in the problem of spatial diffraction is far too restrictive in practice. A more precise estimation of the temporal resolution provided by the system is given by the following expression:

$$\delta t \geq 1/\sqrt{|\ddot{\phi}_t|}. \quad (7)$$

C. Brief Comparison with the Dispersion–Time-Lens Configuration

Time-to-frequency conversion of optical pulses has been previously demonstrated with a system comprising a dispersive medium followed by a time lens, arranged in the appropriate balance.[4–7] A schematic of this configuration is shown in Fig. 2. Specifically, the system must be designed so that the following relation is satisfied:

$$\ddot{\Phi}_\omega \ddot{\phi}_t = 1, \quad (8)$$

where $\ddot{\Phi}_\omega$ is the first-order dispersion coefficient of the dispersive medium (as defined above). If condition (8) is satisfied, then it can be shown that the input–output relation in the system is also given by Eq. (5); i.e., again, the spectrum of the pulse at the output of the system $D(\omega)$ is, within a phase factor $M(\omega)$, proportional to the input temporal waveform $c(t)$ evaluated at the instant $t = \omega/\ddot{\phi}_t$.

Obviously, the main advantage of the configuration proposed herein as compared with the dispersion–time-lens configuration is that our proposal avoids the use of an input dispersive device, and, as a result, it represents a much simpler and practical alternative for implementing time-to-frequency conversion. It is also important to compare the two described configurations for time-to-frequency conversion in terms of the temporal resolutions that they can provide. As discussed above, the temporal resolution corresponding to the single-lens configuration can be estimated from inequality (7). For the dispersion–time-lens configuration, the temporal resolution is limited mainly by the equivalent effects of diffraction arising from the finite aperture. In the temporal context, the aperture corresponds to a finite time window through which the fields pass on their way through the time lens.[2] Briefly, if the input pulse is too short (broadband), it is stretched in excess by the dispersion preceding the time lens and overfills the finite time aperture of the time lens. As mentioned above, this effect essentially limits the achievable temporal resolution, i.e., the shortest pulse that can be processed with the system. Mathematically, the temporal duration of the pulse after dispersion can be estimated as $\Delta t_{\mathrm{out}} \approx |\ddot{\Phi}_\omega|\Delta\omega \approx 2\pi|\ddot{\Phi}_\omega|/\delta t$, where $\Delta\omega$ represents the total bandwidth of the input pulse to the system, and δt represents the fastest temporal feature of this input pulse (temporal resolution). An adequate processing of the pulse is ensured only if its temporal duration after dispersion (i.e., at the input of the time lens) is shorter than the time aperture τ_a of the time lens, $\Delta t_{\mathrm{out}} < \tau_a$. This fixes a limit for the achievable temporal resolution according to the following expression:

$$\delta t > \frac{2\pi}{\tau_a}|\ddot{\Phi}_\omega| \approx \frac{2\pi}{\tau_a}\frac{1}{|\ddot{\phi}_t|}. \quad (9)$$

Note that in deriving inequality (9) we have taken into account the relation between the dispersion and the time-lens phase factor given by Eq. (8). We now have closed-form expressions for the temporal resolution provided by the single-time-lens system [inequality (7)] and by the dispersion–time-lens system [inequality (9)]. Based on these closed-form expressions, the corresponding approaches for time-to-frequency conversion can be now quantitatively compared in terms of achievable temporal resolutions. For the two proposed configurations, the temporal resolution can always be improved (i.e., δt can be shortened) by increasing the magnitude of the phase-factor $|\ddot{\phi}_t|$. [This tendency can be clearly deduced from Eqs. (7) and (9).] In fact, in the single-

time-lens configuration the temporal resolution depends only on this phase-factor $|\ddot{\phi}_t|$, whereas in the dispersion–time-lens system the temporal resolution also depends on the temporal aperture τ_a of the time lens (the longer the time aperture, the faster the temporal feature that can be processed).

For comparative purposes, let us assume that we want to achieve a given temporal resolution δt. In the case of the single-time-lens configuration, the phase-factor $|\ddot{\phi}_t|$ of the time lens must be fixed to ensure that $|\ddot{\phi}_t| > 1/\delta t^2$ [see inequality (7)] whereas in the case of the dispersion–time-lens configuration the phase-factor $|\ddot{\phi}_t|$ of the time lens must be fixed so that $|\ddot{\phi}_t| > 2\pi/(\tau_a \delta t)$ [see inequality (9)]. These requirements indicate that the single-time-lens configuration will require a lower phase factor $|\ddot{\phi}_t|$ (as compared with the dispersion–time-lens configuration) in order to achieve a given temporal resolution δt only if this temporal resolution is slow enough that it satisfies $\delta t > \tau_a/2\pi$. To be able to solve faster temporal features than $\tau_a/2\pi$, the single time lens will require a larger phase factor than the dispersion–time-lens configuration. Thus, based exclusively on time-resolution criteria, in principle, the single-time-lens configuration would be the preferred one for processing pulses with temporal features slower than $\tau_a/2\pi$, whereas the dispersion–time-lens configuration would be more convenient for processing pulses with temporal features faster than $\tau_a/2\pi$. This is only partially true, because it is also important to note that the resolution limit that we are using to compare the systems under study is the fundamental resolution limit of the system; i.e., it is intrinsic to the system configuration itself (ideal system). There are, however, other important aspects that can affect the resolution provided by the described systems, which we did not take into account in our previous discussion. These other aspects include the finite temporal resolution of the final signal recording system, as well as temporal aberrations induced by deviations from the ideal quadratic phase response in the dispersive medium or in the time lens.[9] Regarding these temporal aberrations, it should be mentioned that one of the advantages of using the single-time-lens configuration instead of the conventional dispersion–time-lens approach for time-to-frequency conversion is that we eliminate one of the sources of aberrations in the system, namely, the dispersive medium[9] (as mentioned above, the other source of aberrations is the time lens). Note that the aberrations induced by the dispersive medium (associated with deviations from its ideal quadratic phase spectral response) will become more significant for temporally shorter (spectrally broader) pulses. As a result, it is expected that the elimination of the dispersive medium in the temporal system will have a positive effect on the overall performance of this system (in terms of temporal resolutions). This point nonetheless requires further investigation, but its detailed study is beyond the scope of this work.

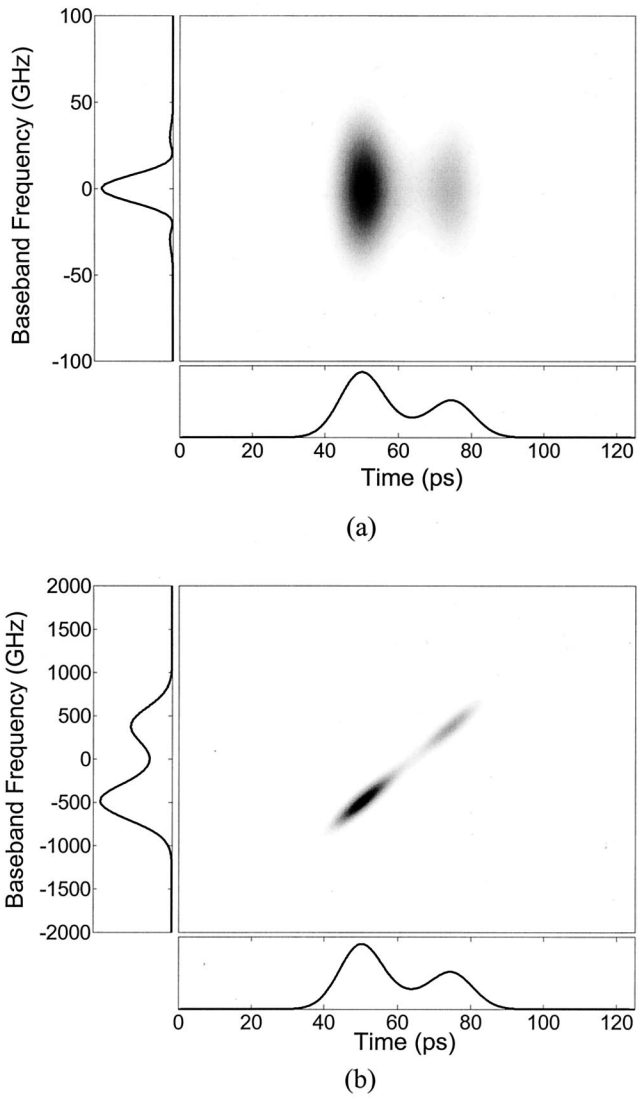

Fig. 3. Simulation results for pulse propagation through a time lens operating within the spectral Fraunhofer regime. Plots at the bottom show the signal in the temporal domain, plots at the left show the signal in the frequency domain, and the larger 2D images show the joint time-frequency representation of the signal. (a) Input pulse to the time lens; (b) output pulse from the time lens.

3. Simulation Results

The introduced theory first has been confirmed by means of numerical simulations. Figure 3 shows results from simulations in which the time lens is configured to operate within the spectral Fraunhofer regime. Specifically, the pulse incident upon the time lens [Fig. 3(a)] and the output pulse from the time lens [Fig. 3(b)] are shown. The plot at the bottom of each figure represents the temporal waveform (average optical intensity), the plot at the left shows the corresponding spectral energy density of the signal, and the contour two-dimensional image shows the joint time-frequency energy distribution of the signal (darker regions in the image correspond to higher intensities). The joint time–frequency representation provides information on the temporal loca-

tion of the signal's spectral components[10] and allows us to get a deeper insight into the structure of the signal itself as well as into the nature of the processes under analysis. For the time–frequency distributions, we have used a combined wideband–narrowband spectrogram,[11] which, in contrast to other distributions, provides good resolution in both time and frequency domains simultaneously without introducing significant interference terms. The input signal [Fig. 3(a)] consists of two consecutive and partially overlapped transform-limited Gaussian pulses of different intensity: each individual pulse has a FWHM time width of ≈8 ps, and the two pulses are separated by ≈25 ps. The total bandwidth of this input signal is estimated to be $\Delta\omega \approx 2\pi \times 100$ GHz. We simulated an ideal time-lens process, i.e., an ideal quadratic phase modulation process. According to inequality (4), to ensure an efficient time-to-frequency mapping, the phase factor of the time lens must satisfy $|\ddot{\phi}_t| \gg \Delta\omega^2/8\pi \approx 15.7 \times 10^3$ rad GHz^2. Specifically, the phase factor of the time lens used in this first simulation is fixed to $\ddot{\phi}_t \approx 22.5 \times 10^4$ rad GHz^2. Note that this value can be achieved with current technology. In particular, phase factors up to $\ddot{\phi}_t \approx 5.623$ THz^2 rad have been reported.[3] Results in Fig. 3 are in excellent agreement with those theoretically predicted. As expected, the energy spectrum of the output pulse [Fig. 3(b)] is a replica (image) of the input pulse temporal shape. Note that the time-lens process does not affect the temporal pulse shape (in intensity). However, the spectral components of the input signal are redistributed in reference to the time axis according to the instantaneous frequency characteristic of the time lens (straight line with a slope equal to the phase factor $\ddot{\phi}_t$). The spectral Fraunhofer condition ensures that this spectral redistribution occurs in such a way that only a single dominant frequency term exists at a given instant of time. This effect can be clearly observed in the time–frequency representation of the output signal in Fig. 3(b): The energy of the signal is distributed in the time–frequency plane along a straight line, corresponding to the instantaneous frequency characteristic of the time lens. This is also consistent with the time–frequency relation between the temporal object and the spectral image defined by relation (5) (this relation is given by the phase factor of the time lens, i.e., by the slope of the instantaneous frequency characteristic). It is worth noting that, as in the case of the real-time Fourier transformation process, the direct correspondence between the time and the frequency domains in the output pulse provides additional capabilities to further control and modify the pulse temporal (spectral) energy distribution (see Ref. 8 for a more detailed discussion on this point).

For comparison, Fig. 4 shows the output signal from a time lens that provides an strength insufficient to ensure time-to-frequency conversion (i.e., the time lens operates out of the spectral Fraunhofer regime), assuming the same input signal as in the previous example. In particular, the time lens used for the simulations in Fig. 4 has a phase factor $\ddot{\phi}_t \approx 2 \times 10^4$ rad GHz^2, which does not satisfy spectral

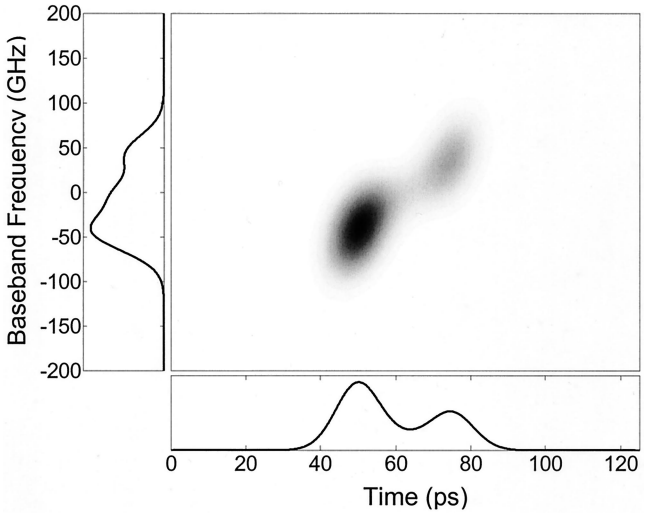

Fig. 4. Simulation results for pulse propagation through a time lens, assuming the same input pulse as in Fig. 3(a) but operating outside the spectral Fraunhofer regime. The representation shows the output pulse from the time lens, with the same definitions as for Fig. 3(a).

Fraunhofer condition (4). In this last case, the spectral components of the signal are again redistributed according to the instantaneous frequency characteristic of the time lens, but the process is now insufficient to ensure an effective separation of these spectral components in the temporal domain (i.e., to ensure an efficient time-to-frequency conversion process). The joint time–frequency representation shows that the output signal energy is distributed in a wider frequency band at each instant of time so that the energy spectrum does not replicate the shape of the temporal waveform.

For completeness, we finally conducted a set of simulations on time-to-frequency conversion by using the conventional dispersion–time-lens configuration. We assume the same input pulse as in the previous examples and the same time lens process as in the last example (Fig. 4). The dispersive medium is designed to fulfill condition (8), i.e. $\ddot{\Phi}_\omega = 1/\ddot{\phi}_t \approx 50$ ps^2/rad. Figure 5 shows the time–frequency representations corresponding to the signal at the output of the dispersive medium [Fig. 5(a)] and the signal at the output of the time lens [Fig. 5(b)]. As expected, the energy spectrum of the output pulse from the system [Fig. 5(b)] is an image of the input pulse temporal shape [Fig. 3(a)]. The use of a dispersive device in the system introduces a significant distortion in the temporal shape of the output pulse as compared with that of the input pulse. In fact, in contrast to the case of the single-time-lens configuration, there is no direct correspondence between the temporal and spectral domains in the output pulse.

4. Experimental Results

Figure 6 shows a schematic of our experimental arrangement used to observe the spectral Fraunhofer regime. An actively mode-locked laser diode with an

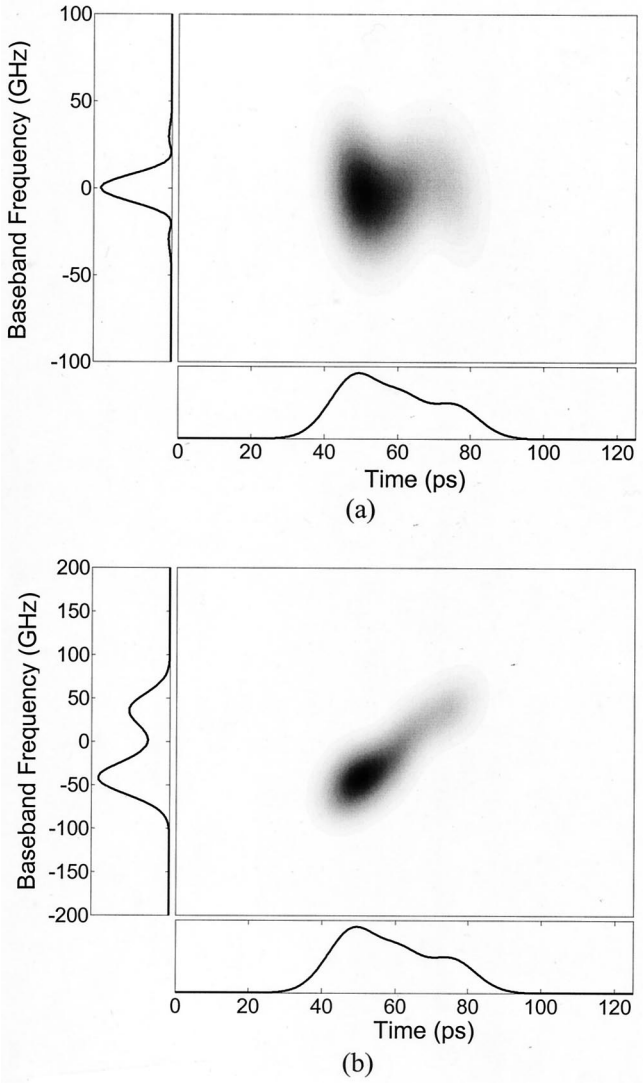

Fig. 5. Simulation results for pulse propagation through a conventional time-to-frequency converter (dispersion–time-lens system) configured to implement time-to-frequency conversion (as shown in Fig. 2), assuming the same input pulse as in Fig. 3(a). (a) Output pulse from the dispersive medium, with the same definitions as for Fig. 3(a). (b) Output pulse from the time lens (system), with the same definitions as for Fig. 3(a).

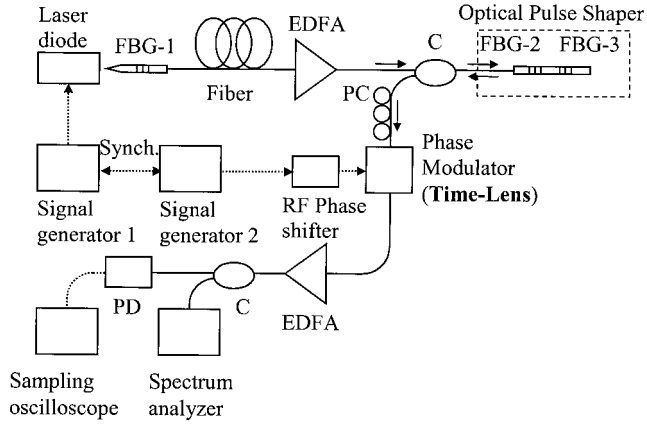

Fig. 6. Schematic of the experimental setup. Solid (dotted) lines are used for optical (electrical) signals. FBG, fiber Bragg grating; EDFA, erbium-doped fiber amplifier; C, fiber coupler; PC, polarization controller; PD, photodetector; Synch, synchronization.

external resonator based on a uniform fiber Bragg grating (FBG-1) was used as the optical pulse source. The source generated optical pulses at a repetition rate of 0.99 GHz centered at a wavelength of 1548 nm. The generated pulses were non-transform-limited (chirped) nearly Gaussian pulses. These pulses were subsequently compressed to a time width of ≈17.5 ps by use of dispersion-compensating fiber. The compressed pulses were conveniently reshaped by means of a FBG-based optical pulse shaper, consisting of two consecutive uniform FBGs (FBG-2 and FBG-3). In particular, the FBGs were specifically designed to generate a nonsymmetric double pulse [see Fig. 7(b)] from the input Gaussian pulses. The gratings FBG-2 and FBG-3 were written in a boron-doped photosensitive fiber by cw UV radiation ($\lambda = 244$ nm) by use of the phase-mask technology. The FBGs were 0.3 mm long and were spaced apart by 0.3 mm. The measured reflectivities of the gratings were 5.3% and 4.8%, respectively. To obtain the desired temporal optical waveform [nonsymmetric double pulse, as shown in Fig. 7(b)], it was necessary to introduce a π phase shift between the reflection coefficients corresponding to the two individual gratings, FBG-2 and FBG-3. For this purpose the grating structure was conveniently processed with UV radiation after its fabrication (i.e., the trimming process). During the measurement stage, the required fine adjustment was achieved by temperature control of the gratings with a thermoelectric module.

A $LiNbO_3$ electro-optic modulator, driven by a sinusoidal RF modulation signal, was used as the time-lens mechanism.[2,4,6] The modulation frequency and modulation index (amplitude) were fixed to $\omega_m = 2\pi 9.9$ GHz rad and $A = 2.4$ rad, respectively. With these values, the phase factor of the time lens can be estimated[2] as $|\ddot{\phi}_t| \approx A\omega_m{}^2 \approx 9286.27$ GHz^2 rad. Note that the two RF signal generators used to drive the mode-locked laser diode and the electro-optic phase modulator (time lens), respectively, were synchronized by means of a signal operating at 10 MHz. We also note that the required synchronization between the incoming optical pulses and the modulation RF signal in the time lens was ensured by use of a RF phase shifter. Finally, the optical signals were measured in the temporal domain with a fast photodetector (PD) followed by a sampling oscilloscope, both providing a bandwidth of ≈50 GHz. For their measurement in the spectral domain, we used a conventional optical spectrum analyzer providing a resolution of $\delta\lambda \approx 0.015$ nm. Figure 7(a) shows the measured energy spectrum of the input pulse (before the time lens). The total bandwidth of the input optical pulse is estimated to be $\Delta\lambda \approx 0.5$ nm ($\Delta\omega \approx 2\pi 62.5$ GHz rad). For the parameters used, the spectral Fraunhofer condition [inequality (4)] is satisfied, but in the form $|\ddot{\phi}_t| > \Delta\omega^2/8\pi$. Figure 7(b) shows the measured energy spectrum

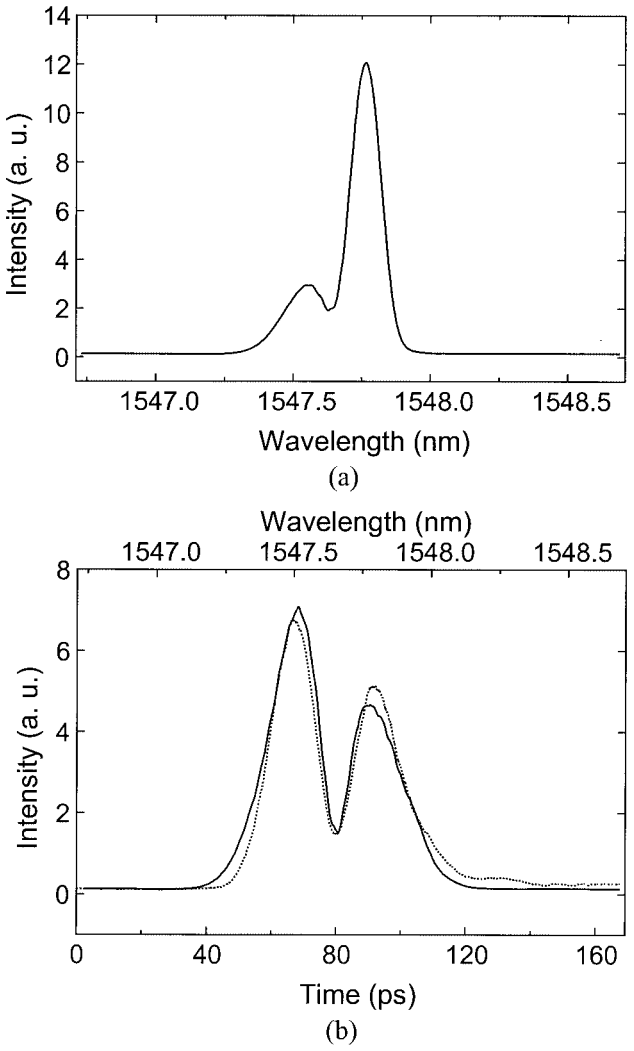

Fig. 7. Experimental results: (a) measured spectrum of the input pulse to the time lens; (b) measured spectrum of the output pulse from the time lens (solid curve, top scale) and measured temporal waveform of the input pulse to (output pulse from) the time lens (dotted curve, bottom scale).

of the output pulse (after the time lens, solid curve). For comparison, the measured temporal waveform of the input (output) pulse is also shown in Fig. 7(b) (dotted curve). The time and wavelength scales in Fig. 7(b) are related according to relation (5) by $t - t_0 \approx -(2\pi c/\lambda_0{}^2\ddot{\phi}_t)(\lambda - \lambda_0)$, where c is the speed of light in vacuum and t_0 and λ_0 are the central instant and the wavelength of the optical pulse, respectively. Our experimental results confirmed our theoretical predictions. As expected, the energy spectrum of the optical pulse at the output of the time lens is an image of the temporal optical waveform at the input of the time lens, according to the relation given by inequality (4). In other words, an efficient time-to-frequency conversion process is achieved. Note that the sign of the time-to-frequency scale conversion is fixed by the sign of the phase factor $\ddot{\phi}_t$; i.e., it depends on the half-period that is chosen for the modulation RF signal in the time lens.

As previously discussed, the temporal resolution provided by our imaging system can be estimated from inequality (7). Specifically, the time lens used in our experiments provides a phase factor $|\ddot{\phi}_t| \approx 9286.27\ \mathrm{GHz}^2$ rad, which fixes a temporal resolution of $\delta t \approx 1/\sqrt{|\ddot{\phi}_t|} \approx 10$ ps. This resolution is of the order of that estimated from our experimental results. Note that the following nonidealities in the system introduce additional errors: (i) the spectral Fraunhofer condition [inequality (4)] is not strictly satisfied; i.e., as mentioned above, it is satisfied as $|\ddot{\phi}_t| > \Delta\omega^2/8\pi$; and (ii) the temporal duration of the input optical pulse ($\approx$75 ps) exceeds the time aperture τ_a of the time lens[2] ($\tau_a \approx 1/\omega_m \approx 16$ ps). As mentioned above, the temporal resolution provided by the system can be improved by increasing the magnitude of the phase factor $|\ddot{\phi}_t|$. In general, alternative technologies for implementing the time lens, such as those based on nonlinear processes,[3,5,7] permit achieving much larger phase factors than the electro-optic technology used herein and consequently have the potential for further improving the achievable temporal resolutions. As an example, a time lens such as that reported in Ref. 3 ($\ddot{\phi}_t \approx 5.623\ \mathrm{THz}^2$ rad) could be used to implement time-to-frequency conversion of optical pulses with a temporal resolution of the order of a few hundreds of femtoseconds [$\approx$420 fs, as determined by inequality (7)].

5. Conclusions

In summary, we have analyzed in detail a new regime (the spectral Fraunhofer regime) in the interaction between optical pulses and time lenses. In this regime the temporal waveform of the input pulse is mapped into the spectral domain by the action of a single time lens. With this idea, simplified and optimized time-to-frequency converters for measuring ultrafast optical waveforms in the spectral domain can be implemented. More importantly, the concepts explored herein should prove to be very useful for other applications in the areas of optical signal processing and optical pulse shaping.

This research was supported by the Fonds de recherche Nature et Technologies of the Québec Government (Canada), by the Division for Research Funds of the Israel Ministry of Science.

References

1. T. Jannson, "Real-time Fourier transformation in dispersive optical fibers," Opt. Lett. **8,** 232–234 (1983).
2. B. H. Kolner, "Space-time duality and the theory of temporal imaging," IEEE J. Quantum Electron. **30,** 1951–1963 (1994).
3. C. V. Bennett and B. H. Kolner, "Upconversion time microscope demonstrating 103× magnification of femtosecond waveforms," Opt. Lett. **24,** 783–785 (1999).
4. M. T. Kauffman, W. C. Banyai, A. A. Godil, and D. M. Bloom, "Time-to-frequency converter for measuring picosecond optical pulses," Appl. Phys. Lett. **64,** 270–272 (1994).
5. E. Arons, E. N. Leith, A.-C. Tien, and R. Wagner, "High-resolution optical chirped pulse gating," Appl. Opt. **36,** 2603–2608 (1997).

6. N. K. Berger, B. Levit, S. Atkins, and B. Fischer, "Time-lens-based spectral analysis of optical pulses by electrooptic phase modulation," Electron. Lett. **36,** 1644–1646 (2000).
7. L. K. H. Mouradian, F. Louradour, V. Messager, A. Barthelemy, and C. Froehly, "Spectro-temporal imaging of femtosecond events," IEEE J. Quantum Electron. **36,** 795–801 (2000).
8. J. Azaña and M. A. Muriel, "Real-time optical spectrum analysis based on the time–space duality in chirped fiber gratings," IEEE J. Quantum Electron. **36,** 517–526 (2000).
9. C. V. Bennett and B. H. Kolner, "Aberrations in temporal imaging," IEEE J. Quantum Electron. **37,** 20–32 (2001).
10. L. Cohen, "Time-frequency distributions—a review," Proc. IEEE **77,** 941–981 (1989).
11. S. Cheung and J. S. Lim, "Combined multiresolution (wide-band/narrow-band) spectrogram," IEEE Trans. Signal Process. **40,** 975–977 (1992).